

A NOVEL DESIGN APPROACH FOR ERBIUM-DOPED FIBER AMPLIFIERS BY PARTICLE SWAM OPTIMIZATION

A. Mowla and N. Granpayeh

Faculty of Electrical Engineering
K. N. Toosi University of Technology
P.O. Box 16315-1355, Tehran 1431714191, Iran

Abstract—A novel design approach for erbium-doped fiber amplifiers is proposed based on particle swarm optimization algorithm. The main six parameters of the EDFAs including: pumping wavelength, input signal power, fiber numerical aperture, erbium-doped area radius, erbium concentration, and the fiber length are optimized utilizing a fast and efficient method called particle swarm optimization algorithm. In this paper, a combination of fiber amplifier bandwidth, gain, and flatness are taken into account as objective function and the results are presented for different pump powers. Our investigation shows that particle swarm optimization algorithm outperforms genetic algorithm in convergence speed, straightforwardness, and coping with high-dimensional spaces, when the parameters of EDFA are to be optimized. It has been shown that the required time for the optimization of the fiber amplifier parameters is reduced four times by using particle swarm optimization algorithm, compared to genetic algorithm method.

1. INTRODUCTION

Erbium-doped fiber amplifiers (EDFAs) are the vital components of the dense wavelength division multiplexing (DWDM) optical communication systems. Current improvements of the DWDM systems and networks are entirely indebted to the EDFAs. Merits of EDFAs are high gain, low noise, broad bandwidth, high output power, and high efficiency of the pump power. Major criterions of the compact optical fiber amplifiers are gain, noise, bandwidth, and gain spectrum flatness. Higher gain and lower noise let the prolongation of the distance between two repeaters, wider bandwidth enables the DWDM networks to embrace more channels that brings about higher capacities,

and flatter gain spectrum causes avoiding transmission impairments due to heterogeneous amplifications. After presenting thorough models for EDFAs that solved propagation and rate equations for a two level laser homogeneous medium [1, 2], tremendous efforts have been made to find the efficient configurations that appease voracious appetite of DWDM systems for higher capacities. Yeh et al. [3] suggested parallel structure of S- and C-band EDFAs with wide 96 nm gain bandwidth of 1480–1576 nm, and Lu et al. [4] proposed a parallel combination of C- and L-band dual-core EDFAs which results in 105 nm bandwidth over 1515–1620 nm. Tellurite-based EDFAs have been investigated to attain flat amplification bandwidth of 76 nm [5]. It is highly desired to reach the same amplification results for EDFAs employed in dynamic DWDM networks, since, adding or dropping channels can cause changes in the gain performance of other existing channels. Therefore, gain-clamping techniques have been proposed. Ring-type optical laser-cavities have been utilized to clamp the gain [6–8]. In addition, gain flattening filters (GFFs), such as fiber Bragg grating (FBG) filters [9–11], dielectric filters, and twin core fiber filters [12] are used to equalize the amplifier gain spectrum. Also, all reflection mirrors (ARMs) or fiber reflection mirrors (FRMs) are used in double-pass structures to enhance the pump efficiency and the amplifier gain [13]. Efficient pumping schemes, such as using a 980 nm and a 1480 nm pump lasers bi-directionally [14] or employing pumping wavelength of 1540 nm [15] and other optimal structures [16], have been presented to modify the gain and noise performances. Martin [17] introduced erbium transversal distribution influence. In consequence, Cheng et al. [18, 19] worked on EDFAs radial effects to earn the most appropriate characteristics.

However, all the aforementioned methods offer worthwhile designs, but they may not work in their best possible configurations, since, too many parameters affect the performance of the EDFAs and for the optimal designs, all of them must be optimized. Not unexpectedly, an optimization algorithm is quite helpful here, in order to find the best global solution. Beside traditional optimization methods, there are some evolutionary computational search algorithms, called global optimization methods (GOMs), that are practical tools to search global maximums and minimums. Genetic algorithm (GA) is one of the most popular GOMs that has been used in diverse fields, recently [22–30]. GA is established upon natural selection and biological behavior of genes [31]. In a nutshell, GA works by evaluating the chromosomes of a random selected population based on their fitness, selecting fittest members of the population, mating the qualified chromosomes to produce offspring, and finally applying mutation to avoid suboptimal solutions. Cheng et al. [18–21] applied this algorithm and offered an

optimal design including radial effects and dual pumped structure. Wei et al. [32] implemented GA algorithm to optimize the multistage EDFAs. On the other hand, Zhang et al. [33], used the improved GA for gain flattening of an ultra wide-band EDFAs by means of stitched long-period fiber gratings (SLPFGs). Also, hybrid GA was used in designing ultra wide-band optical amplifiers [34]. Despite of the effectiveness of GA, it is quite time consuming and needs a large amount of computational works.

Particle swarm optimization (PSO) algorithm is a new and effective method of optimization. This algorithm has been used in solving different engineering problems [35–47]. In this paper, to the best of our knowledge, for the first time we propose the PSO algorithm instead of GA to optimize EDFAs. First, a quick review of PSO is presented. Then, a model of EDFA is given and the parameters of EDFA are optimized by PSO algorithm. In the following, the performance of PSO is compared with that of continuous GA, and it is shown that PSO surpasses GA in speed and simplicity.

2. IMPLEMENTATION OF PSO

Particle swarm optimization algorithm is a global search strategy, first introduced by Kennedy and Eberhart in 1995. The idea was the graphical simulation of the stochastic behavior of the bird flocks, while it resulted in an excellent optimization method [49]. In an n -dimensional space, each group of the n parameters of the function can be considered as a single point. Thus, we can attribute the output values of the function to the points or individuals in the hyperspace. Considering changes over time, these points can be speculated as particles which move, and we can define velocities for particles. In addition, the population is referred to as a swarm, in this method. Particles will be spread in the hyperspace, and according to the values of objective function they are capable of learning from each others to move toward the best point [48]. So, here we have a paradigm of social behavior. The PSO algorithm must enable the particles to modify their movement based on their own best experiences that have ever had, and the success of the particles which have been designated as their neighbors. In this paper, we use star neighborhood structure. In this topology, each particle is a neighbor for all the other particles. New particle position is the sum of its previous position and its current velocity. Also, current particle velocity is the sum of the previous particle velocity, the difference between the best previous particle position and its current position, and the difference between the best position of all particles till now and the current particle position. In

the following, algorithm steps, for global best version of the PSO algorithm, are presented, assuming that our goal is to find the global maximum [49]:

Step 1. Initialize the swarm of particles $P(t)$, somehow that the position of each particle lays stochastically within the hyperspace, $P_i \in P(t)$. P_i and $\bar{x}_i(t)$ refer to a particle and its position, assuming $t = 0$.

Step 2. Evaluate the fitness function F for each particle P_i using its current position $\bar{x}_i(t)$, $F(\bar{x}_i(t))$.

Step 3. Compare the current fitness value of each particle to its best value so far. If $F(\bar{x}_i(t)) > Pbest_i$ then:

- a. $Pbest_i = F(\bar{x}_i(t))$
- b. $\bar{x}_{Pbest_i} = \bar{x}_i(t)$

Step 4. Compare the current fitness value of each particle to the global best particle. If $F(\bar{x}_i(t)) > Gbest_i$ then:

- a. $Gbest_i = F(\bar{x}_i(t))$
- b. $\bar{x}_{Gbest_i} = \bar{x}_i(t)$

Step 5. Renew the velocities of the particles:

$$\bar{v}_i(t) = \varphi \times \bar{v}_i(t-1) + \rho_1 \times C_f(\bar{x}_{Pbest_i} - \bar{x}_i(t)) + \rho_2 \times C_f(\bar{x}_{Gbest_i} - \bar{x}_i(t))$$

where φ is the inertia weight which its value is less than one, parameters ρ_1 and ρ_2 are random values uniformly distributed in $[0, 1]$ and C_f is a positive acceleration constant.

Step 6. Renew the positions of the particles:

- a. $\bar{x}_i(t) = \bar{x}_i(t-1) + \bar{v}_i(t)$
- b. $t = t + 1$

Step 7. Execute the test of convergence, go to *step 2* if convergence does not take place, and finish the search if convergence condition is satisfied.

3. EDFA EQUATIONS AND OPTIMIZATION IMPLEMENTATION

Since optimization is a time consuming process, we need a fast and efficient model for EDFA to simulate its performance. Throughout this work, we adopt the Giles model [1] which is used in most cases of design works. Eliminating the effects of higher levels, a two-level, homogeneously broadened model for Er^{3+} ions are assumed, where the ground level is ${}^4\text{I}_{15/2}$ and the excited level is ${}^4\text{I}_{13/2}$. This two-level model is enough to describe the propagation of optical power in the EDF, because, nearly all of the radiative transitions take place

between these two levels. To work with the continuous spectrum of optical light, we divide the light into optical beams of frequency bandwidth $\Delta\nu_k$ with optical power of P_k centered at frequency ν_k and wavelength λ_k . So, we can consider the propagation equation as N ordinary differential equations, where N is the total number of pump and signal channels. In addition, the rate equation of upper-level ${}^4I_{13/2}$ population of Er^{3+} will be a summation of the emission and absorption contributions of all the light frequency components [19]. Emission and absorption cross sections of Al/P-silica fiber are utilized, which are adopted from Miniscalco investigation [50]. In addition, we choose fiber parameters, somehow, to have V number less than 2.405, so that we will have single mode fiber. Also, we adopt the steady state condition $\partial n_2(r, z, t)/\partial t = 0$ and weakly guiding approximation $\Delta = (n_1 - n_2)/n_2 \ll 1$ to simplify the equations. Therefore, the equation that describes the optical propagation along z -axis is given as follows [19]:

$$\begin{aligned} \frac{dP_k(z)}{dz} = & u_k \sigma_{ek} \int_0^a i_k(r) n_2(r, z, t) [P_k(z) + mh\nu_k \Delta\nu_k] 2\pi r dr \\ & - u_k \sigma_{ak} \int_0^a i_k(r) n_1(r, z, t) P_k(z) 2\pi r dr - u_k l_k P_k(z) \end{aligned} \quad (1)$$

where $P_k(z)$ is the optical power propagating in the core of EDF with frequency ν_k , $u_k = +1$ and $u_k = -1$ demonstrate the forward and backward direction of pump schemes, σ_{ek} and σ_{ak} are the emission and absorption cross sections, a is the fiber radius, i_k is the normalized transverse mode intensity, n_1 and n_2 are the population of Er^{3+} ions in the ground level ${}^4I_{15/2}$ and metastable level ${}^4I_{13/2}$ states, respectively, $mh\nu_k \Delta\nu_k$ specifies the amount of spontaneous emission that takes place from upper level population n_2 while $\Delta\nu_k$ is the effective noise bandwidth, ν_k is the noise power frequency, h is the Planck's constant, and here m is 2, because of the bidirectional ASE, while for pump and signals m is 0. Finally, l_k is the excess fiber loss. This equation is derived for a circularly symmetric fiber.

By solving the rate equations in the steady-state, metastable level population of Er^{3+} ions can be written as:

$$n_2(r, z) = n_t \frac{\sum_k (\tau \sigma_{ak} / h\nu_k) P_k(z) i_k(r)}{1 + \sum_k (\tau (\sigma_{ak} + \sigma_{ek}) / h\nu_k) P_k(z) i_k(r)} \quad (2)$$

where τ is the metastable level lifetime. Note that saturation is involved in this formula, n_t is the erbium-doped concentration $n_t =$

$n_1 + n_2$ and it has a uniform distribution over the core radius a . In addition, the formula of normalized transverse mode intensity considering the fundamental mode inside the core $r < a$ is given as [19]:

$$i_k(r) = \frac{1}{\pi a^2} \left[\frac{v_k J_0(u_k r/a)}{V_k J_1(u_k)} \right]^2 \quad (3)$$

where $V_k = 2\pi a NA/\lambda_k$ is the V number at wavelength λ_k , $NA = \sqrt{n_1^2 - n_2^2}$ is the numerical aperture, and the approximate values for v_k and u_k for $1 \leq V_k \leq 3$ are $v_k = 1.1428V_k - 0.9960$ and $u_k = \sqrt{V_k^2 - v_k^2}$. $J_{0,1}$ are zeroth- and first-order Bessel functions. Also, the following normalization condition must be satisfied:

$$\int_0^a i_k(r) 2\pi r dr = 1 \quad (4)$$

Satisfying this normalization condition ensures us about propagation of total input power in the core radius. Inasmuch as the values of input pump and signal powers are known and we aim to find their output values, here, we have an initial value problem. In the cases of bidirectional pumping and considering back- and forward ASE, we have boundary value problem. Throughout this work, using some approximation, we solve pump, signal, and noise propagation equations as initial value problems, utilizing one-step predictor-corrector method (PCM) [51]. The EDF is divided into small segments and power at each segment is calculated using its own value at previous step and a prediction made at its current step. Similarly, the power is calculated step by step at each frequency. In order to solve Eq. (1) we rewrite it in the form below:

$$\frac{dP_k(z)}{dz} = P_k(z)F_k(z) + C_k(z) \quad (5)$$

where:

$$F_k(z) = u_k[\sigma_{ek} + \sigma_{ak}] \int_0^a i_k(r) n_2(r, z, t) 2\pi r dr - u_k[\sigma_{ak} n_t + l_k] \quad (6)$$

$$C_k(z) = u_k \sigma_{ek} m h \nu_k \Delta \nu_k \int_0^a i_k(r) n_2(r, z, t) 2\pi r dr \quad (7)$$

Utilizing this notation, we can easily solve Eq. (1). Because the light amplification or attenuation has the exponential variations, we

can accept exponential evolutions to simulate power propagations in fiber amplifiers [52]. Accordingly, Eq. (1) can be solved as:

$$P_k(z_{j+1}) = P_k(z_j) \exp((F_k(z_j) + C_k(z_j)/P_k(z_j))\Delta z) \quad (8)$$

where for pump and signal $C_k(z) = 0$, since in these cases $m = 0$.

The pumping wavelength is about 1480 nm, which is adopted for third communication window and is speculated in two-level system. Pumping wavelength of 980 nm is used when the amplifier is assumed to have a three-level model. Step index fiber and uniform distribution of Er^{3+} ions are used in our model to avoid complexity of using graded index fiber and considering radial effects [18]. In the numerical calculations, the data in Table 1 are used. As shown in Table 1, the system has 40 signal channels at frequencies 186.80 to 196.55 THz spaced 250 GHz/channel. Also, ASE noises are calculated at these channels. One forward pump is chosen to pump the amplifier while more than one pump in both directions can be included. Core radius $a = 4.1 \mu\text{m}$, to conform with current fiber data of Lucent technology products [19]. The range of the Er-doped radius b is smaller than that of fiber core.

Table 1. Data required in numerical calculations.

| | |
|-------------------------------------|--------|
| Upper level life time (ms) | 10 |
| Input pump power (mW) | 50 |
| Step distance (m) | L/60 |
| Cladding index | 1.445 |
| Fiber core radius (μm) | 4.1 |
| Excess fiber loss (dB/m) | 0.03 |
| Start frequency (THz) | 186.80 |
| End frequency (THz) | 196.55 |
| Number of channels | 40 |
| Frequency steps (THz) | 0.25 |

Solving Eqs. (5)–(8), EDFA characteristics are known. Fitness function is defined by using the amplifier characteristics as following equation:

$$F = \Delta + \alpha G_c - \beta F_f \quad (9)$$

where Δ is 3 dB bandwidth while the middle hollow of the gain spectrum is neglected. G_c is the central signal gain at wavelength 1550 nm that must be maximized. G_c can be defined at other wavelengths, when we want to work in other bands like S- and L-band. F_f is the difference between the maximum and the average values of the signal gains in the bandwidth, which is included to have flatter gain spectrum. α and β (nm/dB) are the weighting factors. We define fitness function in some way that includes bandwidth, gain, and flatness. Based on the situation, weighting factors are evaluated. Here we assume $\alpha = \beta = 1$. Now we consider the fitness function F as sub-program for the main PSO program. Main program is written according to the algorithm described in the previous section. First, the main program spreads the points or the particles over the parameter ranges. Afterwards a sub-program provides fitness values by use of Eq. (9). Then the main program amends particle positions in each cycle to reach better fitness values. Therefore, throughout this evolutionary process, the global maximum will be found. Continuous PSO is used in this investigation and values of parameters, involved in optimization process, are chosen randomly over the ranges in Table 2. These reasonable ranges are chosen in some way to include likely optimum values according to the existing results in this context.

Table 2. Ranges of parameters, chosen randomly, in the optimization algorithm.

| | |
|--|-------------------------|
| Pumping wavelength λ_p (nm) | 1450–1500 |
| Numerical aperture NA | 0.056287–0.16886 |
| Erbium-doped radius a (μm) | 1.5–4.1 |
| Input signal power P_s (μW) | 1–10 |
| Er^{3+} concentration n_t | $(1-30) \times 10^{24}$ |
| Fiber length L (m) | 2–50 |

4. RESULTS AND DISCUSSIONS

Table 3 contains the results of the particle swarm optimization of EDFA for different pumping powers. In the modeling computer program, pumping power is a constant value. When the pumping power increases, the central signal gain will increase consequently and there is almost a linear relation between pumping power and the central signal gain. Optimal bandwidth will be nearly the same for different pumping

powers with a little drop when pumping power increases. Optimized signal gain spectrum and its associated NF spectrum are shown in Fig. 1(a) for 50 mW pumping power. Also, optimal central signal gains, fiber lengths, Er^{3+} concentrations, and pumping wavelengths are shown in Fig. 1(b) vs. five tested pumping powers. As it is obvious, central signal gains and Er^{3+} concentrations must increase with pumping power while fiber lengths and pumping wavelengths must decrease. If we took Er^{3+} concentration as a constant value, fiber length would increase when the pumping power increases [20, 21]. Optimal input signal power converges to minimum value over its range that results in the highest possible gain spectrum whereas optimal Er^{3+}

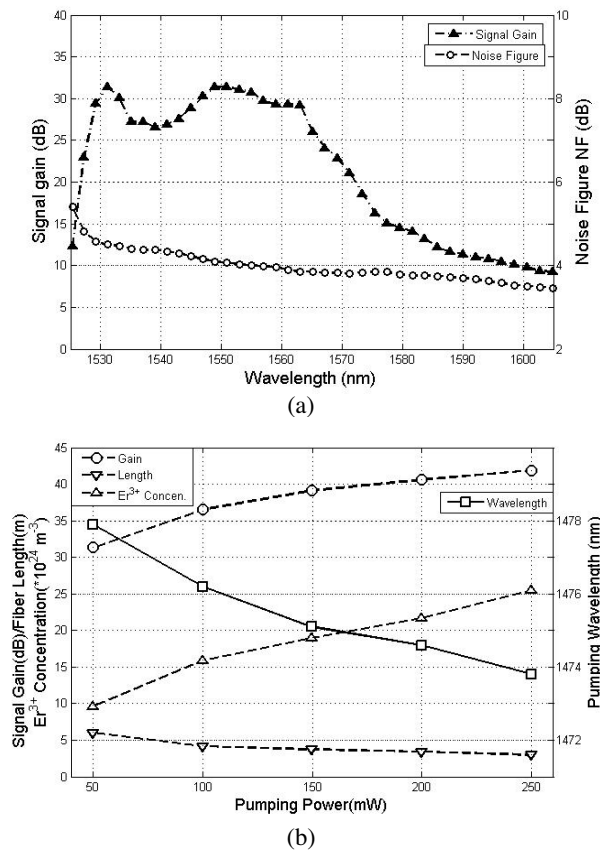


Figure 1. (a) Optimized signal gain spectrum and noise figure for 50 mW pumping power and (b) Values of central signal gains, fiber lengths, Er^{3+} concentrations, and pumping wavelengths vs. pumping powers.

doped radius approaches its maximum value over its range, that is the fiber core radius, to use all of the pumping power. In the case of $b = a$, where a is one of the variables of optimization, optimized a will be too small, less than $1 \mu\text{m}$, which the fiber can easily be damaged by high power pumps and also when a is small, NA will attain a high value that causes higher dispersion distortions. Since the value of a is constant NA does not have a great influence on the results.

It is natural to have nuances between results obtained by different global searching methods when the number of parameters is high, but these slight differences are negligible. The information we need to run the optimization program are given in Table 4. While in genetic algorithm, we need a large number of initial chromosomes to start the algorithm, it is not necessary in PSO to have a large number of particles. The state of being dynamic in PSO is higher than that of GA and each of the particles in PSO are able to find their ways based on their memories of themselves and their neighbors. Both GA and PSO are evolutionary population-based search methods that use a combination of rules to move from a set of points to other ones which are most likely the better positions. In contrast to GA, PSO has memory and is able to utilize the past events. This history of the best solutions is an important key in modifying the positions of particles.

Convergence times of PSO and GA algorithms are compared in Fig. 2. In this figure, the averages of fitness values pertaining to particles of PSO and chromosomes of GA are plotted versus normalized time and it can be seen that required time of convergence in PSO is much less than that of GA. Continuous GA with 80 chromosomes is used whereas its mutation and crossover rates are 0.5 and 0.7, respectively. Choosing inertia weight and acceleration constant in PSO

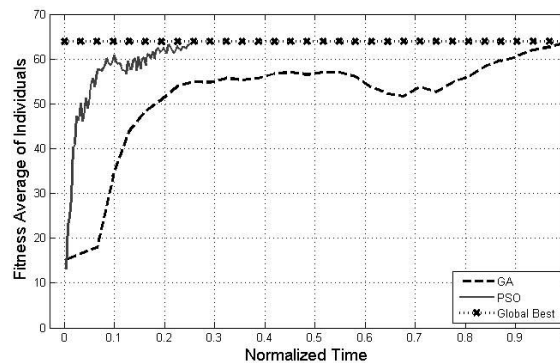


Figure 2. Convergence time comparison of PSO and GA.

Table 3. Results of the particle swarm optimization of the EDFA for different pumping powers.

| | | | | | |
|---|--------|--------|--------|--------|--------|
| Pumping power P_p (mW) | 50 | 100 | 150 | 200 | 250 |
| Optimal pumping wavelength λ_p (nm) | 1477.9 | 1476.2 | 1475.1 | 1474.6 | 1473.8 |
| Optimal numerical aperture NA | 0.1630 | 0.1138 | 0.1165 | 0.1225 | 0.1596 |
| Optimal erbium-doped radius b (μm) | 4.1 | 4.1 | 4.1 | 4.1 | 4.1 |
| Optimal input signal power P_s (μW) | 1.0 | 1.0 | 1.0 | 1.0 | 1.0 |
| Optimal fiber length L (m) | 5.995 | 4.187 | 3.740 | 3.400 | 3.005 |
| Optimal erbium Con. n_t ($\times 10^{24} \text{ m}^{-3}$) | 9.569 | 15.874 | 18.978 | 21.688 | 25.495 |
| Central signal gain G_s (dB) | 31.34 | 36.55 | 39.01 | 40.61 | 41.87 |
| Bandwidth -3 dB $\Delta\lambda$ (nm) | 34.69 | 34.30 | 34.14 | 34.05 | 33.95 |

Table 4. Required information to run PSO program.

| | |
|----------------------------------|-----|
| Number of particles | 40 |
| Number of iterations | 70 |
| Acceleration constant | 2 |
| Inertia weight φ | 0.4 |
| Initial velocity | 0 |
| Initial personal and global best | 0 |

are of great importance. They must be picked up somehow that let PSO be both converged and able to find the global best. If we assume φ higher than 0.4, the algorithm may diverge and if smaller than 0.4 it may converge too fast that the optimization process falls into local maximum. Also, since the used random function has a uniform distribution, the best value for acceleration constant is 2.

There is evidence that when λ_p increases to the values over 1500 nm, amplifier 3 dB bandwidth will increase dramatically while this

is accompanied with rises in the values of n_t and L . That is because when we increase the pumping wavelength, the gain spectrum also will shift to the higher wavelengths and at the expense of losing gain, the bandwidth in the L-band will increase.

5. CONCLUSION

In the design of EDFAs, many factors such as pumping wavelength, fiber length, fiber core radius, input signal power, fiber numerical aperture, and Erbium concentration have great influences. To find optimum values of these factors, we need a reliable and effective method. Although genetic algorithm can be quite helpful, sometimes it is hard to work with this method because of lengthy computational time and complexity. So, in this paper we have offered and applied a new optimization method which is not only simple and straightforward, but also fast and effective. Using particle swarm optimization algorithm, we have optimized the EDFA parameters for different pumping powers so that we can use these results to design high performance EDFAs.

ACKNOWLEDGMENT

The authors would like to thank Iran Telecommunication Research Center (ITRC) for the financial support of this project.

REFERENCES

1. Giles, C. R. and E. Desurvire, "Modeling erbium-doped fiber amplifiers," *J. Lightwave Technol.*, Vol. 9, No. 2, 271–283, 1991.
2. Saleh, A. A. M., R. M. Jopson, J. D. Evankow, and J. Aspell, "Modeling of gain in erbium-doped fiber amplifiers," *IEEE Photon. Technol. Lett.*, Vol. 2, No. 10, 714–717, 1990.
3. Yeh, C. H., C. C. Lee, and S. Chi, "S- plus C-band erbium-doped fiber amplifier in parallel structure," *Opt. Commun.*, Vol. 241, 443–447, 2004.
4. Lu, Y. B., P. L. Chu, A. Alphones, and P. Shum, "A 105-nm ultrawide-band gain-flattened amplifier combining C- and L-band dual-core EDFAs in a parallel configuration," *IEEE Photon. Technol. Lett.*, Vol. 16, No. 7, 1640–1642, 2004.
5. Yamada, M., A. Mori, K. Kobayashi, H. Ono, T. Kanamori, K. Oikawa, Y. Nishida, and Y. Ohishi, "Gain-flattened tellurite-

- based EDFA with a flat amplification bandwidth of 76 nm," *IEEE Photon. Technol. Lett.*, Vol. 10, No. 9, 1244–1246, 1998.
6. Ahn, J. T. and K. H. Kim, "All-optical gain-clamped erbium-doped fiber amplifier with improved noise figure and freedom from relaxation oscillation," *IEEE Photon. Technol. Lett.*, Vol. 16, No. 1, 84–86, 2004.
 7. Yi, L. L., L. Zhan, C. S. Taung, S. Y. Luo, W. S. Hu, Y. K. Su, and Y. X. Xia, "Low noise figure all-optical gain-clamped parallel C+L band erbium-doped fiber amplifier using an interleaver," *Opt. Express*, Vol. 13, No. 12, 4519–4524, 2005.
 8. Yi, L. L., L. Zhan, W. S. Hu, Q. Tang, and Y. X. Xia, "Tunable gain-clamped double-pass erbium-doped fiber amplifier," *Opt. Express*, Vol. 14, No. 2, 570–574, 2006.
 9. Yi, L. L., L. Zhan, J. H. Ji, Q. H. Ye, and Y. X. Xia, "Improvement of gain and noise figure in double-pass L-band EDFA by incorporating a fiber Bragg grating," *IEEE Photon. Technol. Lett.*, Vol. 16, No. 4, 1005–1007, 2004.
 10. Singh, R., Sunanda, and E. K. Sharma, "Gain flattening by long period gratings in erbium doped fibers," *Opt. Commun.*, Vol. 240, 123–132, 2004.
 11. Liang, T. C. and S. Hsu, "The L-band EDFA of high clamped gain and low noise figure implemented using fiber Bragg grating and double-pass method," *Opt. Commun.*, Vol. 281, 1134–1139, 2007.
 12. Lu, Y. B. and P. L. Chu, "Gain flattening by using dual-core fiber in erbium-doped fiber amplifier," *IEEE Photon. Technol. Lett.*, Vol. 12, No. 12, 1616–1617, 2000.
 13. Hung, C. M., N. K. Chen, Y. Lai, and S. Chi, "Double-pass high-gain low-noise EDFA over S- and C+L-bands by tunable fundamental-mode leakage loss," *Opt. Express*, Vol. 15, No. 4, 1454–1460, 2007.
 14. Chang, C. L., L. Wang, and Y. J. Chiang, "A dual pumped double-pass L-band EDFA with high gain and low noise," *Opt. Commun.*, Vol. 267, 108–112, 2006.
 15. Choi, B. H., H. H. Park, and M. J. Chu, "New pumped wavelength of 1540-nm band for long-wavelength-band erbium-doped fiber amplifier (L-band EDFA)," *J. Quantum Electron.*, Vol. 39, No. 10, 1272–1280, 2003.
 16. Pal, M., M. C. Paul, A. Dhar, A. Pal, R. Sen, K. Dasgupta, and S. K. Bhadra, "Investigation of the optical gain and noise figure for multi-channel amplification in EDFA under optimized pump

- condition,” *Opt. Commun.*, Vol. 273, 407–412, 2007.
17. Martin, J. C., “Erbium transversal distribution influence on the effectiveness of a doped fiber: Optimization of its performance,” *Opt. Commun.*, Vol. 194, 331–339, 2001.
 18. Cheng, C. and M. Xiao, “Optimization of an erbium-doped fiber amplifier with radial effects,” *Opt. Commun.*, Vol. 254, 215–222, 2005.
 19. Cheng, C. and M. Xiao, “Optimization of a dual pumped L-band erbium-doped fiber amplifier by genetic algorithm,” *J. Lightwave Technol.*, Vol. 24, No. 10, 3824–3829, 2006.
 20. Cheng, C., Z. Xu, and C. Sui, “A novel design method: A genetic algorithm applied to an erbium-doped fiber amplifier,” *Opt. Commun.*, Vol. 227, 371–382, 2003.
 21. Cheng, C., “A global design of an erbium-doped fiber and an erbium-doped fiber amplifier,” *Opt. Laser Technol.*, Vol. 36, 607–612, 2004.
 22. Yau, D. and S. Crozier, “A genetic algorithm/method of moments approach to the optimization of an RF coil for MRI applications-theoretical considerations,” *Progress In Electromagnetics Research*, PIER 39, 177–192, 2003.
 23. Lucci, L., R. Nesti, G. Pelosi, and S. Selleri, “Phase centre optimization in profiled corrugated circulator horns with parallel genetic algorithms,” *Progress In Electromagnetics Research*, PIER 46, 127–142, 2004.
 24. Meng, Z. Q., “Autonomous genetic algorithm for functional optimization,” *Progress In Electromagnetics Research*, PIER 72, 253–268, 2007.
 25. Ngo Nyobe, E. and E. Pemha, “Shape optimization using genetic algorithms and laser beam propagation for the determination of the diffusion coefficient in a hot turbulent jet of air,” *Progress In Electromagnetics Research B*, Vol. 4, 211–221, 2008.
 26. Zhai, Y. W., X. W. Shi, and Y. J. Zhao, “Optimized design of ideal and actual transformer based on improved micro-genetic algorithm,” *J. of Electromagn. Waves and Appl.*, Vol. 21, No. 13, 1761–1771, 2007.
 27. Chen, X., D. Liang, and K. Huang, “Microwave imaging 3-D buried object using parallel genetic algorithm combined with FDTD technique,” *J. of Electromagn. Waves and Appl.*, Vol. 20, No. 13, 1761–1774, 2006.
 28. Lu, Y. Q. and J. Y. Li, “Optimization of broadband top-load antenna using micro-genetic algorithm,” *J. of Electromagn. Waves*

- and Appl.*, Vol. 20, No. 6, 793–801, 2006.
29. Tian, Y. B. and J. Qian, "ultraconveniently finding multiple solutions of complex transcendental equations based on genetic algorithm," *J. of Electromagn. Waves and Appl.*, Vol. 20, No. 4, 475–488, 2006.
 30. Tu, T. C. and C. C. Chiu, "Path loss reduction in an urban area by genetic algorithm," *J. of Electromagn. Waves and Appl.*, Vol. 20, No. 3, 319–330, 2006.
 31. Haupt, R. L. and S. E. Haupt, *Practical Genetic Algorithms*, John Wiley & Sons, Chap. 2, 3, 2004.
 32. Wei, H., Z. Tong, and S. Jian, "Use of a genetic algorithm to optimize multistage erbium-doped fiber amplifier system with complex structures," *Opt. Express*, Vol. 12, No. 4, 531–544, 2004.
 33. Zhang, A. P., X. W. Chen, J. H. Yan, Z. G. Guan, S. He, and H. Y. Tam, "Optimization and fabrication of stitched long-period gratings for gain flattening of ultrawide-band EDFAs," *IEEE Photon. Technol. Lett.*, Vol. 17, No. 12, 2559–2561, 2005.
 34. Liu, X. and B. Lee, "Optimal design for ultra-broad-band amplifier," *J. Lightwave Technol.*, Vol. 21, No. 12, 3446–3455, 2003.
 35. Li, W. T., X. W. Shi, L. Xu, and Y. Q. Hei, "Improved GA and PSO culled hybrid algorithm for antenna array pattern synthesis," *Progress In Electromagnetics Research*, PIER 80, 461–476, 2008.
 36. Lu, Z. B., A. Zhang, and X. Y. Hou, "Pattern synthesis of cylindrical conformal array by the modified particle swarm optimization algorithm," *Progress In Electromagnetics Research*, PIER 79, 415–426, 2008.
 37. Huang, C. H., C. C. Chiu, C. L. Li, and K. C. Chen, "Time domain inverse scattering of a two-dimensional homogenous dielectric object with arbitrary shape by particle swarm optimization," *Progress In Electromagnetics Research*, PIER 82, 381–400, 2008.
 38. Chamaani, S., S. A. Mirtaheri, M. Teshnehlab, M. A. Shoorehdeli, and V. Seydi, "Modified multi-objective particle swarm optimization for electromagnetic absorber design," *Progress In Electromagnetics Research*, PIER 79, 353–366, 2008.
 39. Li, W. T., X. W. Shi, and Y. Q. Hei, "An improved particle swarm optimization algorithm for pattern synthesis of phased arrays," *Progress In Electromagnetics Research*, PIER 82, 319–332, 2008.
 40. Mahmoud, K. R., M. El-Adawy, S. M. M. Ibrahim, R. Bansal, and S. H. Zainud-Deen, "A comparison between circular and hexagonal array geometries for smart antenna systems using particle swarm

- optimization algorithm,” *Progress In Electromagnetics Research*, PIER 72, 75–90, 2007.
41. Li, W. T., L. Xu, and X. W. Shi, “A hybrid of genetic algorithm and particle swarm optimization for antenna design,” *PIERS Online*, Vol. 4, No. 1, 56–60, 2008.
 42. Zainud-Deen, S. H., W. M. Hassen, E. M. Ali, K. H. Awadalla, and H. A. Sharshar, “Breast cancer detection using a hybrid finite difference frequency domain and particle swarm optimization techniques,” *Progress In Electromagnetics Research B*, Vol. 3, 35–46, 2008.
 43. Lim, T. S., V. C. Koo, H. T. Ewe, and H. T. Chuah, “A SAR autofocus algorithm based on particle swarm optimization,” *Progress In Electromagnetics Research B*, Vol. 1, 159–176, 2008.
 44. Lee, K. C., C. W. Huang, and W. H. Chen, “Analysis of nonlinear microwave circuits by particle swarm algorithm,” *J. of Electromagn. Waves and Appl.*, Vol. 21, No. 10, 1353–1365, 2007.
 45. Lim, T. S., V. C. Koo, H. T. Ewe, and H. T. Chuah, “High-frequency phase error reduction in SAR using particle swarm of optimization algorithm,” *J. of Electromagn. Waves and Appl.*, Vol. 21, No. 6, 795–810, 2007.
 46. Lee, K. C. and J. Y. Jhang, “Application of particle swarm algorithm to the optimization of unequally spaced antenna arrays,” *J. of Electromagn. Waves and Appl.*, Vol. 20, No. 14, 2001–2012, 2006.
 47. Chen, T. B., Y. L. Dong, Y. C. Jiao, and F. S. Zhang, “Synthesis of circular antenna array using crossed particle swarm optimization algorithm,” *J. of Electromagn. Waves and Appl.*, Vol. 20, No. 13, 1785–1795, 2006.
 48. Kennedy, J. and R. C. Eberhart, *Swarm Intelligence*, Chap. 7, Academic Press, 2001.
 49. Engelbrecht, A. P., *Fundamental of Computational Swarm Intelligence*, Chap. 16, John Wiley & Sons, 2005.
 50. Miniscalco, W. J., “Erbium-doped glasses for fiber amplifiers at 1500 nm,” *J. Lightwave Technol.*, Vol. 9, No. 2, 234–250, 1991.
 51. Liu, X. and B. Lee, “A fast and stable method for Raman amplifier propagation equations,” *Opt. Express*, Vol. 11, No. 18, 2163–2176, 2003.
 52. Marhic, M. E. and D. E. Nikonov, “Low third-order glass-host nonlinearities in erbium-doped waveguide amplifiers,” *Proceedings of SPIE*, Vol. 4645, 193, 2002.